arXiv:astro-ph/9706032v1 3 Jun 1997

INTERSTELLAR POLARIZATION IN THE TAURUS DARK CLOUDS: WAVELENGTH DEPENDENT POSITION ANGLES AND CLOUD STRUCTURE NEAR TMC–1

D. W. Messinger, D. C. B. Whittet and W. G. Roberge

Department of Physics, Applied Physics, and Astronomy, Rensselaer Polytechnic Institute, Troy, NY 12180

To appear in the Astrophysical Journal, Sept. 20, 1997, vol 487

ABSTRACT

Systematic variations with wavelength in the position angle of interstellar linear polarization of starlight may be indicative of multiple cloud structure along the line of sight. We use polarimetric observations of two stars (HD 29647, HD 283809) in the general direction of TMC–1 in the Taurus Dark Cloud to investigate grain properties and cloud structure in this region. We show the data to be consistent with a simple two-component model, in which general interstellar polarization in the Taurus Cloud is produced by a widely distributed cloud component with relatively uniform magnetic field orientation; the light from stars close to TMC–1 suffers additional polarization arising in one (or more) subcloud(s) with larger average grain size and different magnetic field directions compared with the general trend. Towards HD 29647, in particular, we show that the unusually low degree of visual polarization relative to extinction is due to depolarization associated with the presence of distinct cloud components in the line of sight with markedly different magnetic field orientations. Stokes parameter calculations allow us to separate out the polarization characteristics of the individual components. Results are fit with the Serkowski empirical formula to determine the degree and wavelength of maximum polarization. Whereas $\lambda_{\rm max}$ values in the widely distributed material are similar to the average (0.55 μm) for the diffuse interstellar medium, the subcloud in line of sight to HD 283809, the most heavily reddened star in our study, has $\lambda_{\rm max} \approx 0.73$ μm, indicating the presence of grains $\sim 30\%$ larger than this average. Our model also predicts detectable levels of circular polarization toward both HD 29647 and HD 283809.

Subject headings: ISM: dust, extinction — polarization — ISM: magnetic fields — ISM: individual (Taurus Cloud) — Stars: individual (HD 29647, HD 283809, HD 283812)

1. INTRODUCTION

The dark cloud complex in Taurus provides a particularly suitable laboratory in which to study the properties of interstellar dust grains in quiescent environments. As it is relatively nearby ($\sim$ 140 pc) and $\sim 20^\circ$ from the Galactic plane, extinction in this area of sky arises almost exclusively within the cloud itself (Elias 1978; Straižys & Meistas 1980; Kenyon, Dobrzycka & Hartmann 1994). The physical and chemical properties of both the dust and gas are reasonably well constrained. The cloud has a filamentary structure (e.g., Cernicharo et al. 1985), containing embedded dense cores detected in line emission of gas phase molecules such as NH_3 and CS (e.g., Myers & Benson 1983; Zhou et al. 1989). The cores have typical masses of a few $M_\odot$, gas temperatures of $\sim 10\,K$, and densities $\sim 10^4\,cm^{-3}$ (e.g., Wilson & Minn 1977), and are active sites of low-mass star formation (e.g., Lada et al. 1993). A discontinuity between dust properties in the outer layers and dense inner regions of the cloud has been demonstrated. Grains in the outer layers (at visual extinctions $A_V < 3$) have optical properties similar to those of dust in the diffuse interstellar medium (Vrba & Rydgren 1985; Kenyon et al. 1994), whereas infrared spectroscopy demonstrates the presence of icy mantles on the grains in regions of higher extinction (Whittet et al. 1988, 1989; Chiar et al. 1995).

As in other regions of the interstellar medium (ISM), polarization of background starlight in the Taurus dark cloud (TDC) is caused by the alignment of spinning grains with respect to the ambient magnetic field (see Roberge 1996 for a recent review of the physics of grain alignment). The rapid Larmor precession of the grains' angular momenta about magnetic field lines results in alignment correlated with the direction of the magnetic field (Martin 1971). Observations of linear polarization may thus be used to map the magnetic field in the plane of the sky; results for the TDC (Moneti et al. 1984; Tamura et al. 1987; Myers & Goodman 1991; Goodman et al. 1990, 1992) show that the distribution of polarization vectors is fairly uniform over the entire cloud on a macroscopic scale. However, Goodman et al. (1995) cautioned that maps of optical polarization may not be indicative of conditions deep within molecular clouds if the grains in high-density regions are not efficient polarizers. Gerakines, Whittet, & Lazarian (1995) showed that the polarization efficiency, p/A, decreases rapidly with increasing extinction within the TDC. This general trend might be caused by sensitivity of the alignment mechanism to physical conditions; however, it could also be due, at least in part, to depolarization effects associated with small-scale structure within the cloud. The relationship between polarization measurements, magnetic field and cloud structure is therefore of great importance to our understanding of cloud fragmentation, collapse, and star formation.

A good candidate for the study of depolarization effects associated with small-scale structure is the line of sight to the reddened B-type star HD 29647 (see Table 1 for basic information and references). Fortuitously, this star lies behind the outer regions of the TMC–1 condensation within the dark cloud (Crutcher 1985). Depolarization in this line of sight is suggested by the fact that the degree of linear polarization is much less than expected for the degree of extinction, compared with other stars in the region (Whittet et al. 1992). The polarization measurements also show significant rotation of the position angle with wavelength (by 23° between 0.35 and 2.0 μm; see Figure 1b), a phenomenon most naturally explained in terms of the presence of two or more cloud components with differing grain size distributions and magnetic field directions (Coyne 1974). Another star behind TMC–1, HD 283809, shows similar but less extreme behavior.

In this paper, we analyze the wavelength dependence of polarization towards HD 29647 and HD 283809 with reference to a 'control' star

(HD 283812) with 'normal' polarization properties. First, we describe the nature of the region and summarize previous work on the optical properties of the dust in the line of sight. The method of analysis is described in § 3. Results are presented and discussed in § 4, and our conclusions are summarized in § 5.

2. DESCRIPTION OF THE REGION

HD 29647 lies at a distance of 170 ± 20 pc, and therefore appears to be situated just behind the TDC region at 140 ± 10 pc (Crutcher 1985). Contributions from foreground and background material are likely to be small, the visual extinction of the star ($A_V \approx 3.7$) arising almost entirely within the TDC itself. The line of sight to HD 29647 intersects Heiles Cloud 2 within the TDC at a point $\sim 8'$ north of the northernmost clump of dense molecular gas in TMC–1 (see Figure 1 of Crutcher 1985). Schloerb & Snell (1984) describe Heiles Cloud 2 as a rotating ring that is fragmenting as it collapses, and interpret TMC–1 as a dense filament resulting from this collapse[1]. Observations of ^{13}CO line emission at the position of HD 29647 clearly reveal the presence of two distinct components, at radial velocities of 5.1 and 6.5 km/s relative to the LSR (see Schloerb & Snell 1984 and Crutcher 1985; the spectrum in the upper left frame of Schloerb & Snell's Figure 4 corresponds to the position of HD 29647). Data for molecules such as CN, HCN and HCO$^+$, which trace denser material, are consistent in velocity with the 5.1 km/s component, which is therefore assumed to correspond to clump material. These observations strongly support our adoption of a two-component model, such as a clump embedded in lower density material, for the dust towards HD 29647. HD 283809 lies in the same general region ($\sim 6'$ SE of HD 29647) and has substantially higher extinction ($A_V \sim 5.8$), suggesting a greater contribution from the clump. Unfortunately, no detailed information on molecular line velocities is available specific to this line of sight.

The wavelength dependence of interstellar extinction in the TDC has been studied in the visible and near infrared by several authors (Straižys, Wisniewski & Lebofsky 1982; Straižys, Černis & Hayes 1985; Vrba & Rydgren 1985; Kenyon et al. 1994; Whittet et al. 1997), with generally consistent results. Stars with relatively low extinctions ($A_V < 3$) have normal extinction curves, characterized by values of the ratio of total to selective extinction ($R_V = A_V/E_{B-V}$) close to the average of 3.1 for diffuse regions of the ISM. HD 29647 and HD 283809 have values of R_V (Table 1) somewhat above this average, indicating a trend towards larger average particle size. This is consistent with the presence of denser material in these lines of sight, in which grain growth processes become more rapid. The extinction curve of HD 29647 shows more dramatic differences in the ultraviolet compared with the average for the diffuse ISM (Cardelli & Savage 1988). The mid-ultraviolet extinction bump centered near 2175 Å is substantially broader, weaker, and shifted to shorter wavelength, whereas the amplitude of the far ultraviolet extinction rise is relatively high. The origin of these differences is not well understood, but it seems likely that growth processes in dense material along the line of sight have somehow modified and/or depleted the carrier of the bump. No information is available on the extinction curve of HD 283809 in the satellite ultraviolet. However, Straižys et al. (1985) find appreciable differences between HD 283809 and HD 29647 in the blue to near ultraviolet, leading them to conclude that the properties of the small-grain population are different in these lines of sight despite their proximity in the sky.

The wavelength dependence of interstellar polarization in the TDC has been studied by Whittet et al. (1992, 1997). Results are well characterized by the 'Serkowski law' (Serkowski 1973; Serkowski, Mathewson & Ford 1975; Wilking et al. 1980, 1982; Whittet et al. 1992; see § 3 below). Values of the wavelength of maximum polarization, $\lambda_{\rm max}$, which is sensitive to the size of the aligned grains, typically lie in the range 0.5–0.6 μm for stars with $A_V < 3$, consistent with the mean value of 0.55 μm found in the diffuse ISM. Thus, the aligned grain population seems to behave normally in lines of sight lacking dense material, consistent with normal values of R_V determined in the same extinction range. HD 283809 and (especially) HD 29647 have higher $\lambda_{\rm max}$ values (see Table 1), consistent with the presence of larger grains in the clump component.

---

[1] Tamura et al. (1987) review other explanations for the velocity structure in the line of sight, which include the possibility of local disturbances resulting from a shock wave or cloud-cloud collision.

We adopt the A2 V star HD 283812 as the control for our study of interstellar polarization towards HD 29647 and HD 283809. There are several reasons why HD 283812 is a suitable standard. It is situated $\sim 45'$ SE of HD 29647 and HD 283809, in a region devoid of strong molecular emission. It has relatively low visual extinction ($A_V \approx 1.9$), yet is quite highly polarized: the polarization efficiency, $p_{\rm max}/A_V \approx 3.3$ %/mag, is close to the maximum value observed anywhere in the ISM, indicating a lack of depolarization effects associated with complex magnetic field structure or multiple cloud components (Gerakines et al 1995). Low/normal values of R_V and $\lambda_{\rm max}$ (Table 1) indicate that grain properties in the line of sight seem to be typical of the diffuse ISM. Most importantly, there is an absence of any detectable rotation with wavelength in the position angle of polarization towards HD 283812 (see Table 1 and Figure 1b): the standard deviation σ_θ in the mean is comparable with the observational uncertainty ($\sim 1^\circ$) in the individual measurements, and the slope $d\theta/d\lambda$ of a linear fit to the $\theta(\lambda)$ plot is not significantly different from zero. The mean position angle $< \theta >$ is consistent with the general trend of polarization vectors on the sky, which runs approximately NE–SW, as illustrated in Figure 2. More generally, this map strongly suggests the existence of a relatively uniform layer of polarizing dust permeating the region. The degree, position angle and wavelength-dependence of polarization towards HD 283812 are similar to those of other stars obscured by this layer (e.g., compare data for HD 283812 and Elias 19 in Whittet et al. 1992). Taking all of these factors into consideration, we conclude that HD 283812 is a reliable probe of grain properties in the extended layer; we assume HD 29647 and HD 283809 to have additional extinction arising in local concentrations where grain and magnetic field properties are different.

3. ANALYSIS

3.1. Data and Empirical Fits

The observational data used for this analysis consist of broadband linear polarimetry (p, θ) in eight standard passbands between 0.35 and 2.0 μm for each of the three program stars, taken from Whittet et al. (1992). The reader is referred to that paper for details of the individual measurements and discussion of data acquisition and reduction procedures. Plots of the degree, $p(\lambda)$, and position angle, $\theta(\lambda)$, of polarization against λ^{-1} appear in Figure 1. Empirical fits to the data based on the Serkowski formula

$$\frac{p(\lambda)}{p_{\rm max}} = \exp\left\{-K \ \ln^2\left(\frac{\lambda_{\rm max}}{\lambda}\right)\right\} \qquad (1)$$

allow evaluation of the parameters $p_{\rm max}$ (the amplitude of peak polarization), $\lambda_{\rm max}$ (the wavelength at which the peak occurs), and K (sensitive to the width of the polarization curve). Fits performed by Whittet et al. (1992) are plotted in Figure 1a and values of the fit parameters are listed in Table 1.

The polarization curves plotted in Figure 1a and represented by the Serkowski parameters in Table 1 refer to the observed $p(\lambda)$ *integrated over the entire pathlength to each star*. Our analysis below allows us to separate diffuse and dense components towards HD 29647 and HD 283809 and to deduce independent Serkowski curves for the dense component.

3.2. Description of Model

We will test the theory that the lines of sight to HD 29647 and HD 283809 contain distinct dense-cloud components which are responsible for anomalous behavior in the net observed polarization. It seems plausible that these dense regions are condensations embedded in the main TDC complex (although our analysis does not depend on this). A schematic representation of the adopted model is shown in Figure 3. For convenience, we refer to the proposed dense-cloud components in the lines of sight to HD 29647 and HD 283809 as "Cloud 2a" and "Cloud 2b", respectively. Although Clouds 2a and 2b are in all probability physically connected, the optical properties of material along these two lines of sight are not identical (§ 2). The extended cloud layer sampled by HD 283812 is referred to as "Cloud 1", and is assumed to contribute equally to the extinction of all three stars. Thus, whereas the polarization towards HD 283812 is produced only by Cloud 1, the polarization towards HD 29647 is a superposition of the two polarized components (1 and 2a), and similarly HD 283809 (1 and 2b).

3.3. Stokes Parameters

The Stokes parameters, Q and U, are related to the linear polarization, p, by

$$Q/I = p \cos 2\theta \tag{2}$$

and

$$U/I = p \sin 2\theta \tag{3}$$

where p is the degree of linear polarization, θ is the position angle of polarization, and I is the total intensity $I_{\max} + I_{\min}$ (Hall & Serkowski 1963; Whittet 1992).

Our analysis relies on the fact that, for small polarizations, the quantities $q = Q/I$ and $u = U/I$ are additive over individual cloud components. An approximate solution of the transfer equations for partially polarized radiation (Martin 1974) shows that the starlight transmitted by a series of N uniform slabs has Stokes parameters such that

$$q = \sum_{k=1}^{N} p_k \cos 2\theta_k \tag{4}$$

and

$$u = \sum_{K=1}^{N} p_k \sin 2\theta_k, \tag{5}$$

where p_k and θ_k are, respectively, the magnitude and position angle of the polarization that would be observed if only the kth slab were present. The preceding expressions are accurate to order p^2; this is an excellent approximation here, where $p \sim 10^{-2}$.

Applying this result to our two component model, we have

$$q_{obs} = q_1 + q_2 \tag{6}$$

and

$$u_{obs} = u_1 + u_2 \tag{7}$$

where subscript 1 represents Cloud 1 and subscript 2 represent Cloud 2 (a or b). Assuming q_1 and u_1 are given by observations of HD 283812 at a given wavelength, we calculate q_2 and u_2 from the observed polarization towards HD 29647 and HD 283809. This procedure is repeated for each available passband, allowing us to retrieve $p(\lambda)$ and $\theta(\lambda)$ for the dense cloud components in each line of sight.

4. RESULTS

Results of the calculations described in § 3.3 are given in Table 2. The values listed are calculated $p(\lambda)$, $\theta(\lambda)$ for HD 29647 (Cloud 2a) and HD 283809 (Cloud 2b). Uncertainties in the calculated quantities p and θ were determined from the observational uncertainties. It is striking that the calculated $\theta(\lambda)$ for each cloud is almost independent of wavelength to within the calculated error bars (Figure 4b)[2], consistent with our hypothesis that a simple two-component model adequately describes cloud and magnetic field structure along these lines of sight.

Taking a simple weighted average of the θ values in Table 2, we calculate the mean position angle of polarization for the cloud towards HD 29647 (cloud 2a) to be $\theta = 110° \pm 1°$, and similarly, for HD 283809 (cloud 2b), $\theta = 82° \pm 2°$. The dense cloud components for these stars are plotted as dashed lines in the visual polarization map in Figure 2. It is evident that the magnetic field direction in the dense material implied by our calculations is not consistent with the general trend for the extended region ($\theta \sim 30°$); towards HD 29647, it is nearly orthogonal. However, additional support for a substantially larger value for θ in the denser material is provided by near infrared (1.65 μm) polarization measurements for highly obscured field stars in this region, reported by Moneti et al. (1984) (see their Figure 1). In particular, the object Elias 16 ($A_V \sim 20$ mag; Elias 1978) has $\theta \sim 78°$ at 1.65 μm, similar to our calculated value for Cloud 2b.

The calculated $p(\lambda)$ values in Table 2 have the expected form for interstellar polarization and are well-represented by the Serkowski law (equ. 1). Fitting this formula to the data enables us to infer properties of the grain populations within the dense cloud material. Results are shown in Figure 4a, and the fit parameters are listed in Table 3. The data for HD 283812 are shown for comparison. We see that $\lambda_{\rm max}$ values are longer for both Cloud 2a and Cloud 2b compared with Cloud 1 (Table 3), implying proportionately larger average grain radii, as expected for denser material where grain growth is most rapid (e.g., Jura 1980; Whittet 1992). That the largest value of $\lambda_{\rm max}$ occurs towards HD 283809 is consistent with its higher extinction, implying a greater contribution from high density material. The lower peak polarization for Cloud 2b was not anticipated: this suggests that the polarizing grains may not be as efficiently aligned in this region (again consistent with higher density; Goodman et al. 1995; Gerakines et al. 1995), but it could also result from a less favorable magnetic field geometry within the dense cloud. The relatively high observed (net) polarization towards HD 283809 appears to arise predominantly in Cloud 1. Assuming that the dense component contributes extinction $[A_V]_{\rm dense} \sim 3.9$ towards HD 283809 (the difference between the total extinctions of HD 283809 and HD 283812), then the polarization efficiency in the dense material is $[p_{\rm max}/A_V]_{\rm dense} \sim 1.1$, a factor of 3 less than in the diffuse material sampled by HD 283812.

Circular polarization is expected when the direction of grain alignment varies along the line of sight (Martin 1974). To estimate the magnitude V/I of circular polarization predicted by our model, we integrated the radiative transfer equations for the Stokes parameters with respect to distance along each line of sight (Lee & Draine 1985). We adopted a simple geometrical model consisting of three uniform slabs, where the foreground and background slabs represent the large-scale cloud and the intervening slab represents the embedded clump. We modeled the grains as perfectly aligned oblate spheroids composed of astronomical silicate (Draine & Lee 1984), with axial ratios of 2:1 (the shape inferred for aligned grains in nearby molecular clouds; Hildebrand & Dragovan 1995). We assumed, somewhat arbitrarily, that the grains in the foreground and background slabs have radii $a = 0.1$ μm; grains in the middle slab (the dense clump) are assumed to be larger by a factor η, where η is the ratio of $\lambda_{\rm max}$ inferred for the dense clump to that observed in the extended cloud toward HD 283812 (§ 4). In general, imperfect grain alignment and variations in the magnetic field along the line of sight reduce the polarization by a factor $\Phi < 1$

---

[2] The large uncertainty in the calculated angle at 2.04 μm for the line of sight to HD 283809 is due to propagation of the uncertainty of the original measurement at this wavelength.

relative to that observed for perfect grain alignment and a homogeneous magnetic field with the most favorable inclination. For each line of sight, we estimated Φ by comparing the linear polarization computed from our radiative transfer model (§ 4) to the linear polarization observed in the line of sight.

Our calculations of the circular polarization predict detectable levels of circular polarization in the lines of sight toward HD 29647 and HD 283809. For example, in the J (1.2 μm) passband, the calculations described in § 3.4 indicate $V/I \sim 0.04\%$ toward HD 29647 and $\sim 0.6\%$ toward HD 283809. For comparison, Martin & Angel (1976) observe V/I in the range 0.02–0.08% in the near infrared towards several reddened stars. A search for circular polarization toward HD 29647 and HD 238809 would provide a test of our model.

5. CONCLUSION

The observed rotation of the polarization position angle with wavelength towards HD 29647 and HD 283809 is consistent with a two-component model for polarizing material in these lines of sight, in which the net polarization is produced by distinct cloud regions with differing average magnetic field direction and grain size. The most plausible model for the region is a sheet of continuous material extending over much of the Taurus dark cloud, with an embedded dense core (or cores) in the lines of sight to HD 29647 and HD 283809. Analysis based on the Stokes' parameter allows us to estimate the polarization properties of the dense components. The wavelength dependence of linear polarization is shown to be well-represented by the Serkowski empirical formula with $\lambda_{\max} \approx 0.61$ μm (HD 29647) and 0.73 μm (HD 283809), compared with 0.55 μm for the continuous sheet. The position angle of polarization for the dense material towards HD 29647 appears to be almost perpendicular to that of the cloud as a whole. Detectable levels of circular polarization are predicted toward HD 29647 and HD 283809, and a future search for circular polarization in these lines of sight would provide a useful test of our model.

We would like to thank Lida He for the use of his Serkowski fitting program. We also thank Don Mizuno and Sean Carey for assistance with the data analysis package REDUCE used in the creation of the polarization map. This research is funded by NASA grants NAGW-3001 and NAGW-3144.

REFERENCES

Cardelli, J.A., & Savage, B.D. 1988, ApJ, 325, 864

Cernicharo, J., Bacheller, R., & Duvert G. 1985, A&AS, 149, 273

Chiar, J.E., Adamson, A.J., Kerr, T.H., & Whittet, D.C.B. 1995, ApJ, 455, 234

Coyne, G.V. 1974, AJ, 79, 565

Crutcher, R.M. 1985, ApJ, 288, 604

Crutcher, R.M., Troland, T.H., Goodman, A.A., Heiles, C., Kazès, I., & Myers, P.C. 1993, ApJ, 407, 175

Draine, B.T., & Lee, H.M. 1984, ApJ, 285, 89

Elias, J.H. 1978, ApJ, 224, 857

Gerakines, P.A., Whittet, D.C.B., & Lazarian, A. 1995, ApJ, 455, L171

Goodman, A.A., Bastien, P., Myers, P.C., & Ménard, F. 1990, ApJ, 359, 363

Goodman, A.A., Jones, T.J., Lada, E.A., & Myers, P.C. 1992, ApJ, 399, 108

Goodman, A.A., Jones, T.J., Lada, E.A., & Myers, P.C. 1995, ApJ, 448, 748

Hall, J.S., & Serkowski, K. 1963, in Basic Astronomical Data, ed. K.Aa. Strand (Chicago: Univ. of Chicago Press), 293

Hildebrand, R.H., & Dragovan, M. 1995, ApJ, 450, 663

Jura, M. 1980, ApJ, 235, 63

Kenyon, S.J., Dobrzycka, D., & Hartmann, L. 1994, AJ, 108, 1872

Lada, E.A., Strom, K.M., & Myers, P.C. 1993, in Protostars and Planets III, eds. E.H. Levy & J.I. Lunine (Tucson: University of Arizona Press)

Lee, H.M., & Draine, B.T. 1985, ApJ, 290, 211

Martin, P.G. 1971, MNRAS, 153, 279

Martin, P.G. 1974, ApJ, 187, 461

Moneti, A., Pipher, J.L., Helfer, H.L., McMillan, R.S., & Perry, M.L. 1984, ApJ, 282, 508

Myers, P.C., & Benson, P.J. 1983, ApJ, 266, 309

Myers, P.C., & Goodman, A.A. 1991, ApJ, 373, 509

Roberge, W.G. 1996, in ASP Conf. Ser. Vol. 97, Polarimetry of the Interstellar Medium, eds. W.G. Roberge & D.C.B. Whittet (San Francisco, ASP), 401

Schloerb, F.P., & Snell, R.L. 1984, ApJ, 283, 129

Serkowski, K. 1973, in IAU Symp. no. 52, Interstellar Dust and Related Topics, eds. J.M. Greenberg & H.C. van de Hulst (Dordrecht: Reidel), 145

Serkowski, K., Mathewson, D.S., & Ford, V.L. 1975, ApJ, 196, 261

Straižys, V., Černis, K., & Hayes, D.S. 1985, ApSS, 112, 251

Straižys, V., & Meistas, E. 1980, Acta. Astron., 30, 541

Straižys, V., Wisniewski, W.Z., & Lebofsky, M.J. 1982, ApSS, 85, 271

Tamura, M., Nagata, T., Sato, S., & Tanaka, M. 1987, MNRAS, 224, 413

Vrba, F.J., & Rydgren, A.E. 1985, AJ, 90, 1490

Whittet, D.C.B. 1992, Dust in the Galactic Environment (Bristol: IoP Publishing)

Whittet, D.C.B., Adamson, A.J., Duley, W.W., Geballe, T.R., & McFadzean, A.D. 1989, MNRAS, 241, 707

Whittet, D.C.B., Bode, M.F., Longmore, A.J., Adamson, A.J., McFadzean, A.D., Aitken, D.K., & Roche, P.F. 1988, MNRAS, 233, 321

Whittet, D.C.B., Gerakines, P.A., He, L., & Hough, J.H. 1997, in preparation

Whittet, D.C.B., Martin, P.G., Hough, J.H., Rouse, M.F., Bailey, J.A., & Axon, D.J. 1992, ApJ, 386, 562

Wilking, B.A., Lebofsky, M.J., Martin, P.G., Rieke, G.H., & Kemp, J.C. 1980, ApJ, 235, 905

Wilking, B.A., Lebofsky, M.J., & Rieke, G.H. 1982, AJ, 87 695

Wilson, T.L., & Minn, Y.K. 1977, A&A, 54, 933

Zhou, S., Wu, Y., Evans, N.J., Fuller, G.A., & Myers, P.C. 1989, ApJ, 346, 168

This 2-column preprint was prepared with the AAS LaTeX macros v4.0.

Fig. 1.— Observed spectral dependence of polarization (degree and position angle) towards HD 29647 (squares), HD 283809 (circles) and HD 283812 (triangles). The curves fit to the $p(\lambda)$ data (Figure 1a) are based on the Serkowski formula (equation 1) with $p_{\max}$, $\lambda_{\max}$ and K treated as free parameters. The lines in Figure 1b are linear least squares fits to $\theta(\lambda)$.

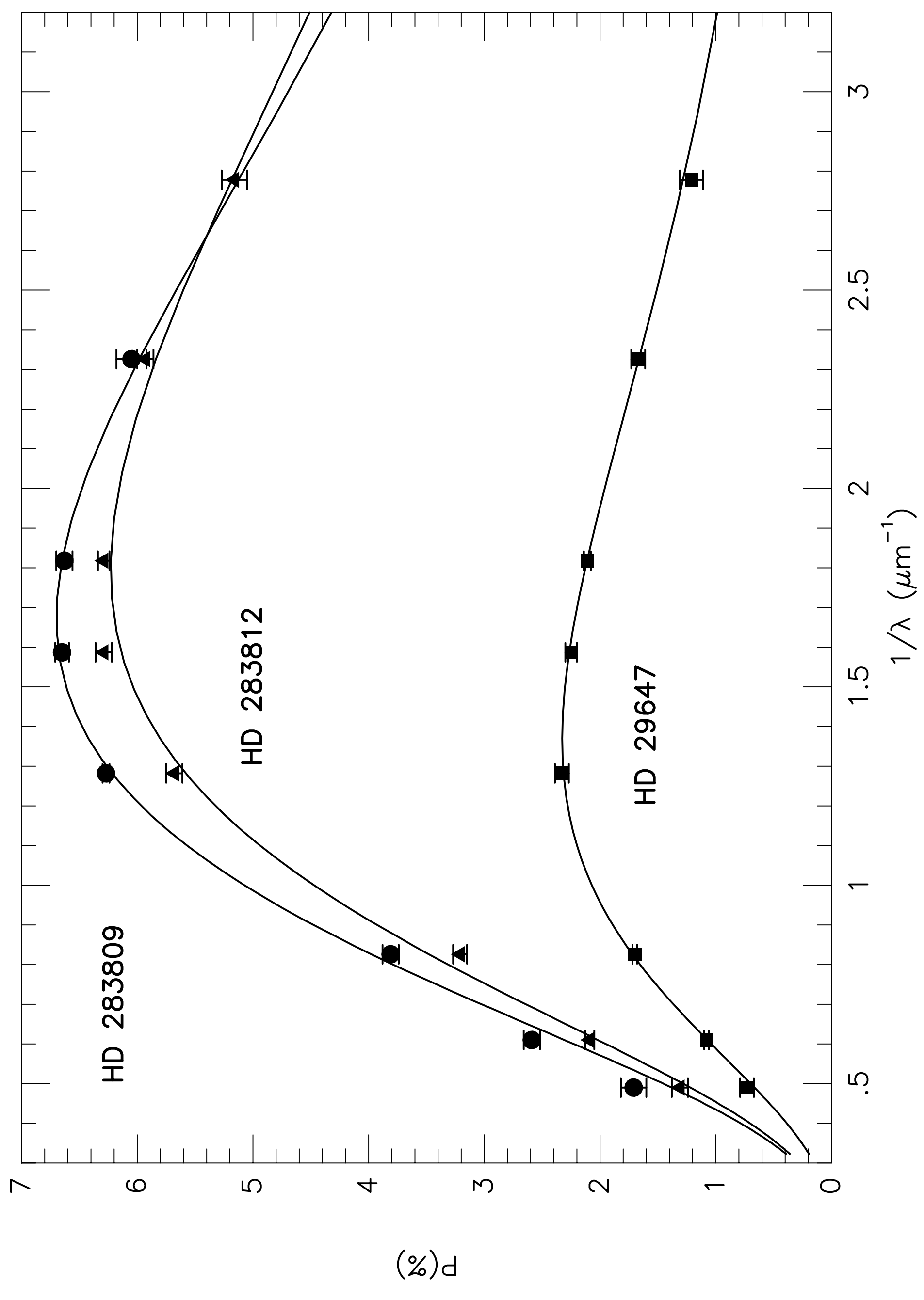

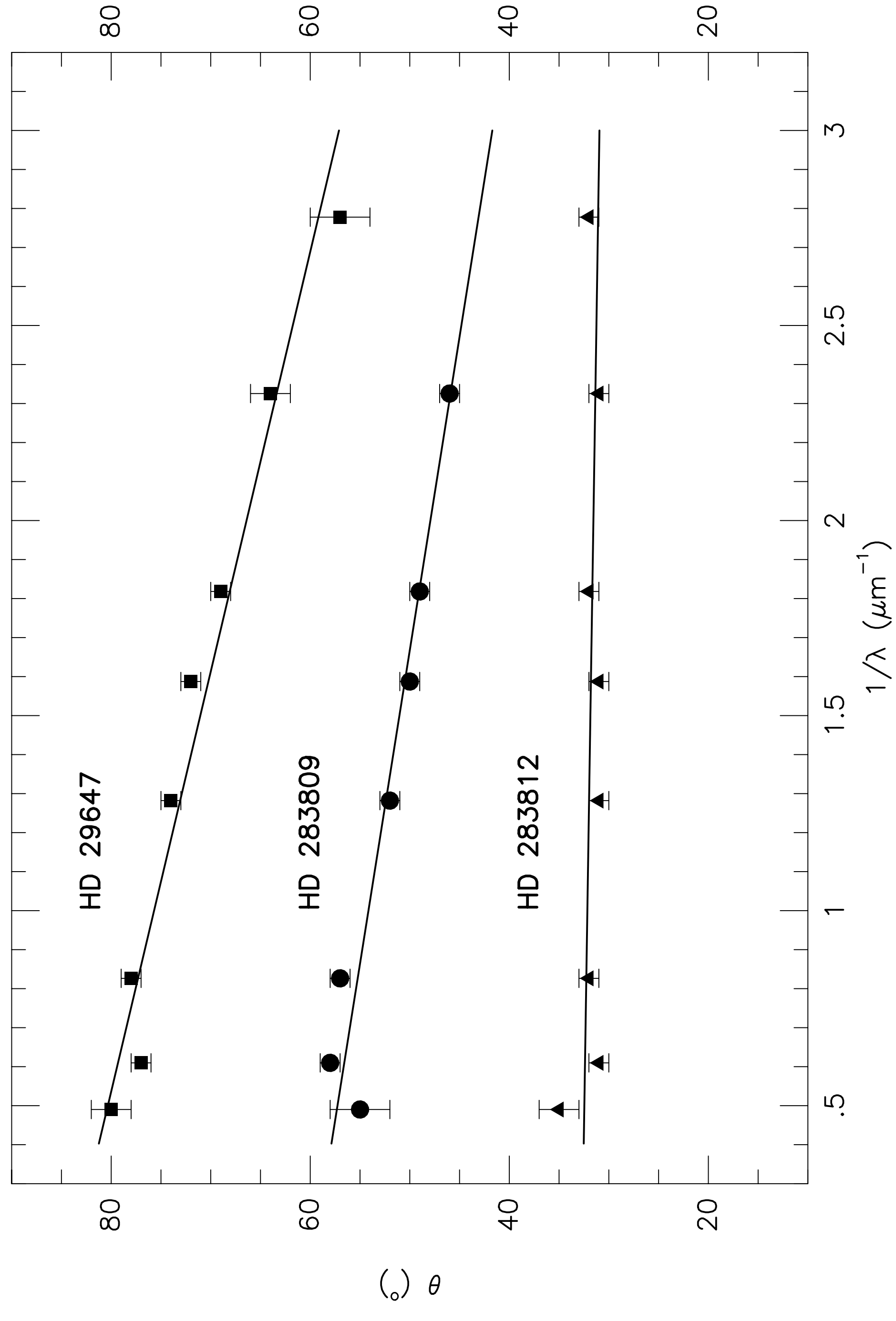
HD 29647
HD 283809
HD 283812
θ (°)
80
60
40
20
1/λ (μm^{-1})
.5
1
1.5
2
2.5
3

Fig. 2.— Linear polarization map of the Taurus dark cloud region surrounding HD 29647. Field stars from Moneti et al. (1984) are denoted by + signs and their visual polarization vectors represented by solid lines. The stars HD 29647, HD 283809 and HD 283812 (in sequence from North to South) are plotted as filled circles using data from Whittet et al. (1992). Observations of the line of sight, and calculated values for the modeled clumps to HD 29647 and HD 283812 (see text), are represented by solid and dashed lines, respectively.

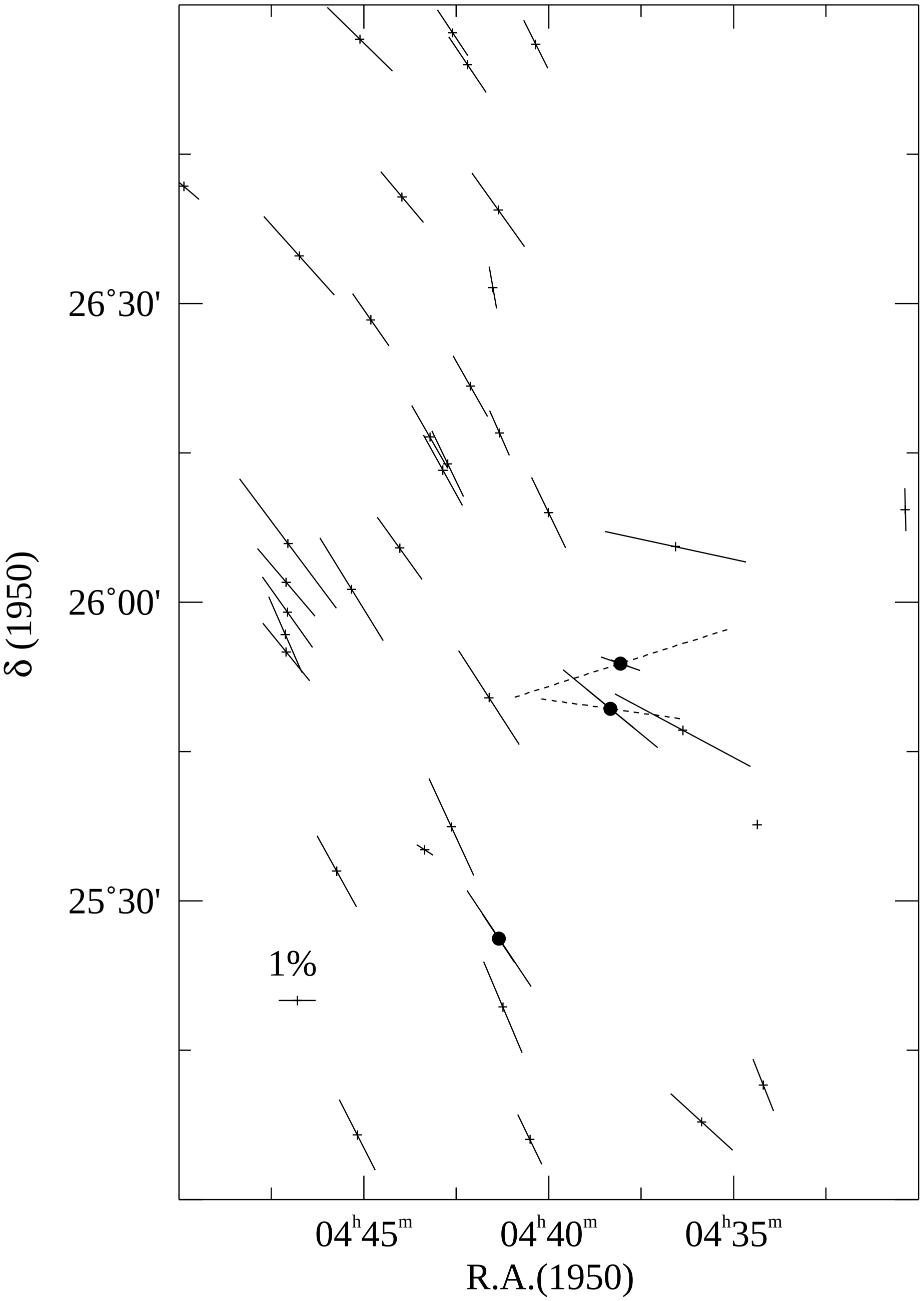

Fig. 3.— Schematic representation of our model for the TMC–1 region, in which a continuous sheet of material (sampled by HD 283812, Cloud 1) contains denser embedded concentrations. Dense material towards HD 29647 and HD 283809 is labelled Cloud 2a and Cloud 2b, respectively.

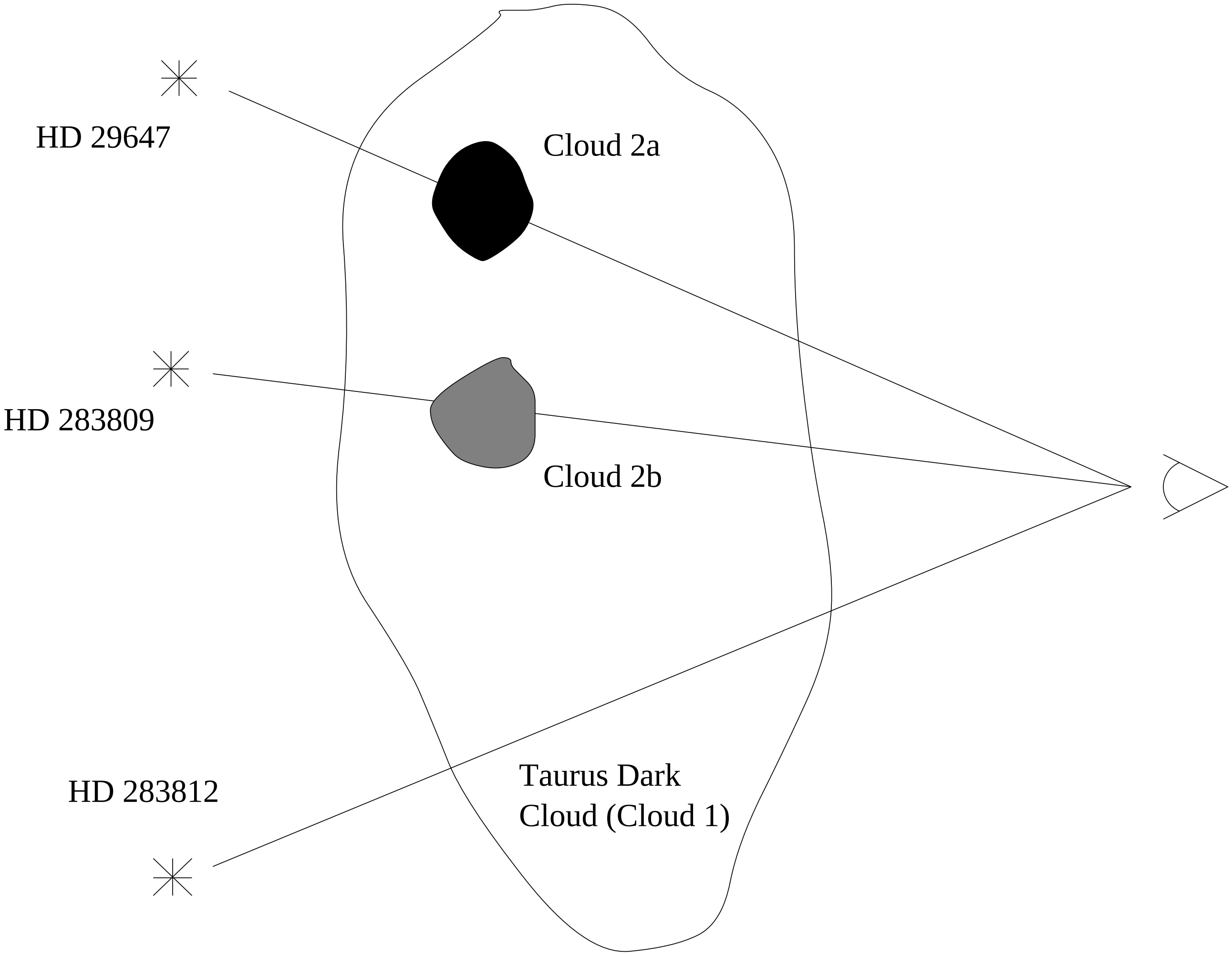

Fig. 4.— Similar to Figure 1, but showing calculated polarization data (degree and position angle) towards HD 29647 (Cloud 2a) and HD 283809 (Cloud 2b). Data for HD 283812 (Cloud 1) are shown for comparison. The parameters of the Serkowski curves fit to $p(\lambda)$ are given in Table 3.

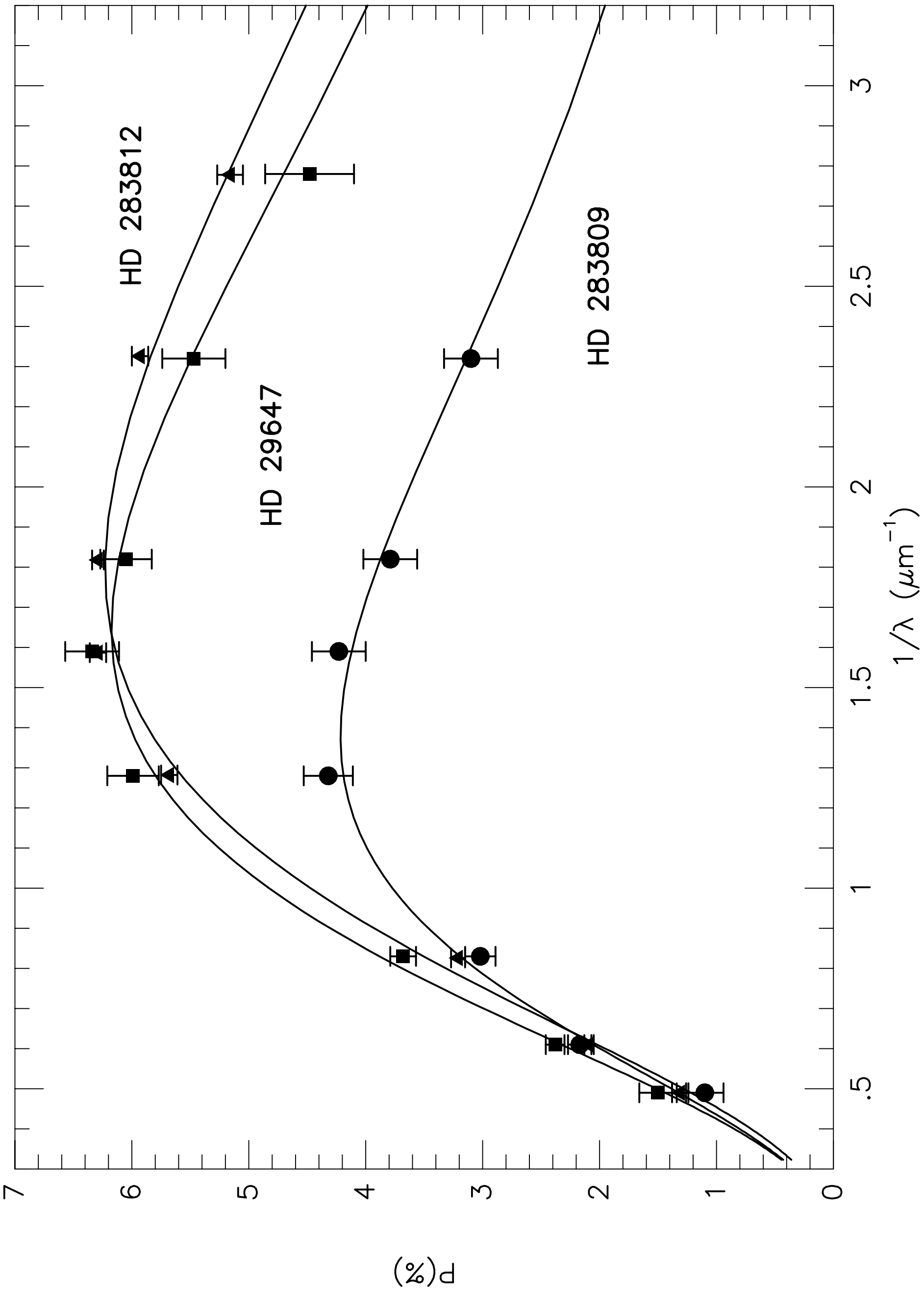

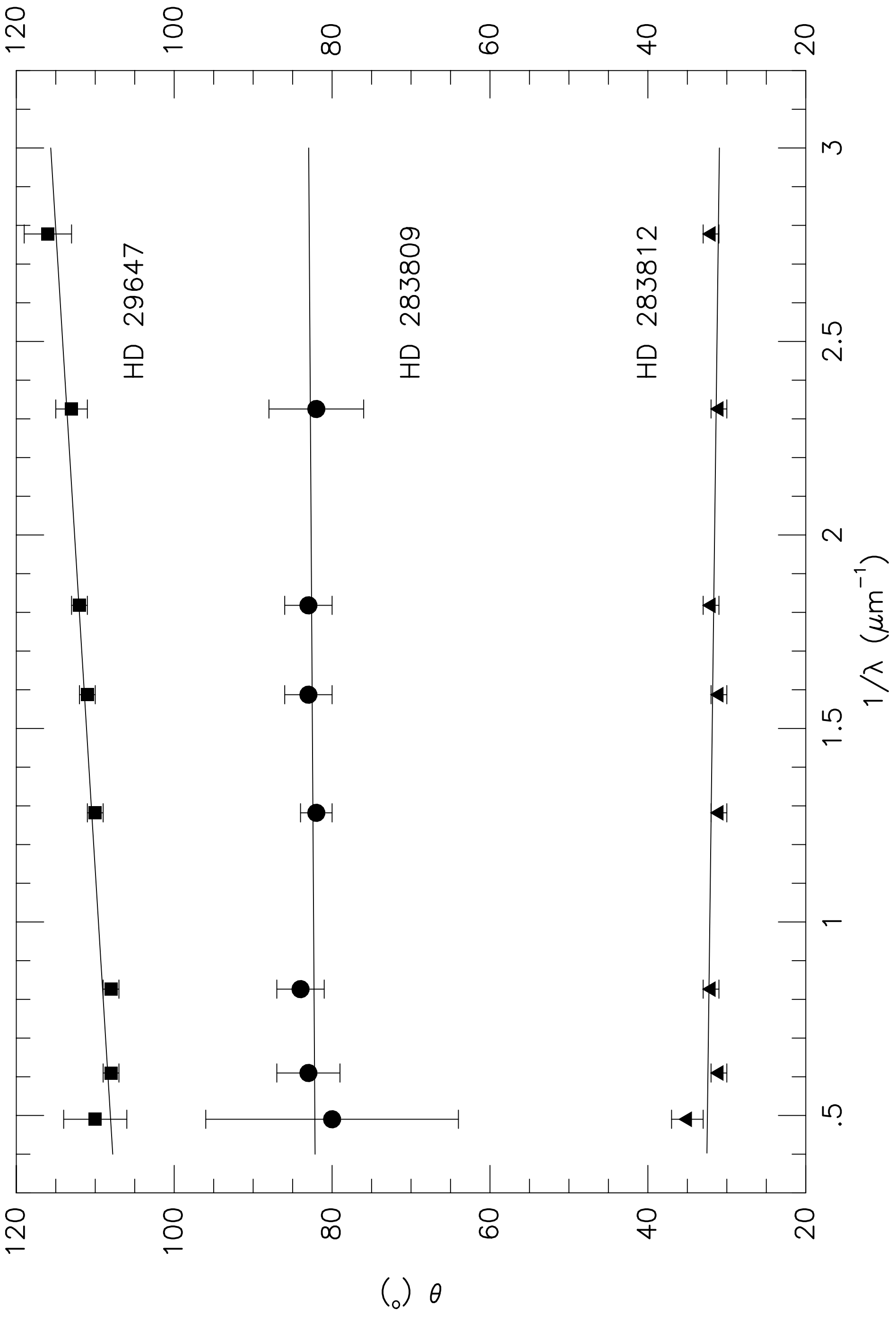
HD 29647
HD 283809
HD 283812
θ (°)
1/λ (μm^{-1})
120
100
80
60
40
20
.5
1
1.5
2
2.5
3

Table 1: SPECTRAL TYPE, EXTINCTION AND POLARIZATION DATA FOR THE PROGRAM STARS

	HD 29647	HD 283809	HD 283812
Spectral Type	B6-7 IV[a]	B3 V[b]	A2 V[c]
E_{B-V}	1.00[a]	1.61[b]	0.66[c]
R_V [d]	3.62	3.58	2.87
$p_{\max}$ (%)[e]	2.30	6.70	6.30
$\lambda_{\max}$ (μm)[e]	0.73	0.59	0.55
K [e]	1.15	0.97	0.96
$< \theta >$ (°)[e]	73.5	52.0	31.6
σ_θ(°)[e]	7.8	4.4	1.4
$d\theta/d\lambda$ (°/μm)[e]	13.9	7.3	2.4

---

[a] Vrba & Rydgren 1985; Crutcher 1985.

[b] Straižys et al. 1985.

[c] Straižys & Meistas 1980.

[d] Gerakines et al. 1995.

[e] Whittet et al. 1992.

Table 2: CALCULATED LINEAR POLARIZATIONS FOR CLOUD COMPONENTS 2a AND 2b

	HD 29647 (Cloud 2a)				HD 283809 (Cloud 2b)			
λ (μm)	p (%)	δp (%)	θ (°)	$\delta\theta$ (°)	p (%)	δp (%)	θ (°)	$\delta\theta$ (°)
0.36	4.48	0.38	116	3				
0.43	5.47	0.27	113	2	3.10	0.23	82	6
0.55	6.05	0.22	112	1	3.79	0.23	83	3
0.63	6.34	0.23	111	1	4.23	0.23	83	3
0.78	5.99	0.22	110	1	4.32	0.21	82	2
1.21	3.68	0.11	108	1	3.02	0.13	84	3
1.64	2.38	0.08	108	1	2.17	0.10	83	4
2.04	1.50	0.16	110	4	1.10	0.19	80	16

Table 3: SERKOWSKI FIT PARAMETERS FOR HD 283812 (CLOUD 1), HD 29647 (CLOUD 2a) AND HD 283809 (CLOUD 2b)

Parameter	HD 283812 (Cloud 1)	HD 29647 (Cloud 2a)	HD 283809 (Cloud 2b)
$p_{\max}$	6.30 ± 0.07	6.17 ± 0.24	4.22 ± 0.25
$\lambda_{\max}$	0.55 ± 0.01	0.61 ± 0.04	0.73 ± 0.05
K	0.96 ± 0.05	0.99 ± 0.15	1.08 ± 0.24